

Joint state-parameter estimation for a control-oriented LES wind farm model

B.M. Doekemeijer[†], S. Boersma[†], L.Y. Pao[‡], J.W. van Wingerden[†]

[†] Delft Center for Systems and Control, Delft University of Technology, The Netherlands

[‡] Faculty of Electrical Engineering, University of Colorado Boulder, United States

E-mail: b.m.doekemeijer@tudelft.nl

Abstract. Wind farm control research typically relies on computationally inexpensive, surrogate models for real-time optimization. However, due to the large time delays involved, changing atmospheric conditions and tough-to-model flow and turbine dynamics, these surrogate models need constant calibration. In this paper, a novel real-time (joint state-parameter) estimation solution for a medium-fidelity dynamical wind farm model is presented. In this work, we demonstrate the estimation of the freestream wind speed, local turbulence, and local wind field in a two-turbine wind farm using exclusively turbine power measurements. The estimator employs an Ensemble Kalman filter with a low computational cost of approximately 1.0 s per timestep on a dual-core notebook CPU. This work presents an essential building block for real-time wind farm control using computationally efficient dynamical wind farm models.

1. Introduction

With the expected growth in our population from 7 billion in 2017 to over 9 billion by 2040, a rapid urbanization that “adds a city the size of Shanghai to the world’s urban population every four months” [1], and a global economy with an average growth rate of 3 – 4% per year [2], the rising demand for energy is not foreseen to slow down any time soon. With the global awakening on climate change, there is a shift from fossil fuel reserves towards renewable energy sources, among which wind energy plays an important role. Though, in many areas of the world, fossil fuels continue to be less expensive than renewable energy sources, slowing down this necessary change in our choice of energy sources.

To make wind energy more financially competitive with non-renewable alternatives, wind turbines are being placed together in wind farms to reduce installation and maintenance costs [3]. However, challenges arise due to the formation of wakes. Wakes are slower, more turbulent regions of air flow, formed downwind of the turbine rotor due to the extraction of energy. In the Lillgrund offshore wind farm, turbines operating in the wake of another experience losses in power capture of up to 23% compared to individually placed turbines, thereby limiting potential cost reductions in wind farms [4]. The area of wind farm control aims to reduce the levelized cost of wind energy¹ through coordinated operation of the turbines inside a wind farm, accounting for these wake effects.

Currently, wind turbines inside a farm are operated in a locally greedy fashion. Doing so, the turbine rotor is yawed perpendicular to the mean wind direction, while the generator torque

¹ The levelized cost of energy is a measure to compare the economical expenses of different energy sources.

and blade pitch angles are regulated to optimize power extraction and to mitigate fatigue loads. However, high-fidelity simulations [5–7], wind tunnel experiments [7–9], and field tests [10] have shown serious potential in purposely misaligning the rotor plane with the wind direction in order to laterally deflect the wake away from downstream-standing turbines. This so-called “wake redirection control” has situationally shown to increase the wind farm’s power production by 10 – 15%. Further, purposely derating turbines inside a farm has shown potential for wind farms to meet a demanded power reference signal provided by, e.g., a transmission system operator [11–13]. This so-called “active power control” may make wind farms viable for providing ancillary grid services, a topic that will become increasingly important as the share of renewable energies in the electricity supply increases.

Wind farm control research typically relies on computationally efficient, surrogate models that accurately predict the flow and turbine dynamics inside the wind farm.² However, no such model exists according to the best of the authors’ knowledge, due to the lack of knowledge about the environment, the complex dynamics of wind on a range of temporal and spatial scales, and the variability of atmospheric conditions (see [3] for an overview of the state-of-the-art control and control-oriented modeling for wind farms). Furthermore, accurate dynamical models such as large-eddy simulation (LES) models are nonlinear and computationally expensive, making them intractable for controller synthesis. On the other hand, computationally inexpensive models are often steady-state, only accurate for a limited set of atmospheric conditions, and therefore require real-time calibration. Therefore, the wind farm control problem calls for a closed-loop control solution, as visualized in Fig. 1.

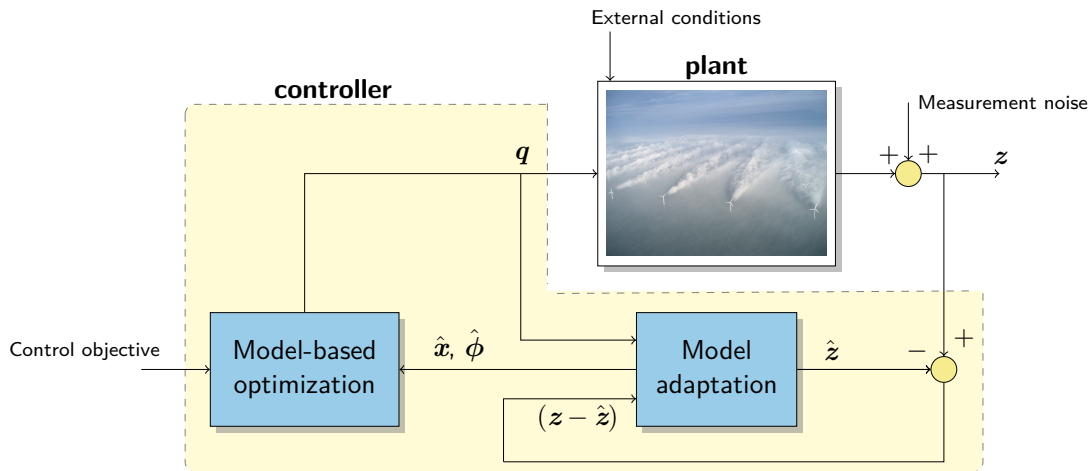


Figure 1: Closed-loop wind farm control framework. Measurements z (e.g., from SCADA or lidar systems) are fed into the controller. First, parameters in the surrogate wind farm model \hat{x} and $\hat{\phi}$ are adapted to the actual conditions inside the farm. Using the calibrated model, an optimization algorithm determines the control policy q for all turbines (e.g., yaw angles, blade pitch angles). This may be a set of constant operating points, but can also be time-varying, depending on whether the surrogate model is time-varying, and the optimization method used.

This paper presents a time-efficient joint state-parameter estimation (“model calibration”) algorithm for the medium-fidelity dynamical model “WindFarmSimulator” (WFSim) [14]. This calibration solution allows wind farm control algorithms relying on WFSim (e.g., [15]) to deal with time-varying atmospheric conditions and model discrepancies, while maintaining

² Model-free methods exist, but they typically go paired with slow convergence rates, and their applicability in practice remains uncertain [3]. The remainder of this paper is limited to model-based wind farm control methods.

computational efficiency. This paper builds on previous work [16,17] by including the estimation of inflow (freestream) conditions and adaptation of the turbulence model to the present conditions, which vary in time due to atmospheric fluctuations and changes in turbine operation. Fundamentally, we move from state-only estimation to joint state-parameter estimation.

The structure of this paper is as follows. Firstly, the WFSim model is described in Section 2. Secondly, the adaptation algorithm is discussed in Section 3. Thirdly, a case study is presented demonstrating the potential of this algorithm in Section 4. The paper is concluded in Section 5.

2. WindFarmSimulator

WFSim is a dynamical wind farm model developed at the Delft University of Technology for the purpose of real-time wind farm control. A summary of WFSim is given here, and the interested reader is referred to [14]. The model is derived from the three-dimensional unsteady Navier-Stokes equations, simplified to 2D (at hub height) under some modifications to the continuity equation, to better represent the flow of three-dimensional LES. Furthermore, turbines are modeled using actuator disk theory, and an adjusted version of Prandtl’s mixing length turbulence model is implemented. Within this turbulence model, the mixing length parameter has been made a linearly increasing function of the downstream distance, as suggested by [18]. The equations are solved after temporal and spatial discretization. A snapshot of the flow field from a two-turbine simulation in WFSim is shown in Figure 2.

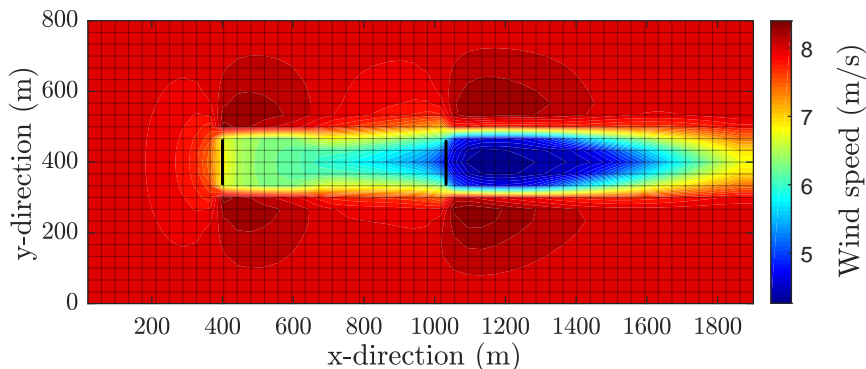


Figure 2: A two-turbine simulation in the WFSim model, with inflow from the left. The wireframe indicates the spatial grid upon which the flow and pressure fields are resolved.

Mathematically, the WFSim model can be represented by the following dynamical system:

$$\begin{aligned} \mathbf{x}_{k+1} &= f(\mathbf{x}_k, \mathbf{q}_k, \phi_k), \\ \mathbf{z}_k &= g(\mathbf{x}_k, \mathbf{q}_k), \end{aligned} \tag{1}$$

where $\mathbf{x}_k \in \mathbb{R}^N$ is the model state vector at time instant k , containing the longitudinal wind speed, lateral wind speed, and pressure term at every point of the spatial grid. The control inputs $\mathbf{q}_k \in \mathbb{R}^{2N_T}$ are the yaw angles γ and thrust coefficients C_T of each turbine, with N_T the number of turbines. The yaw angle has a direct physical relationship to the turbine, while the latter is a non-dimensionalized value of the axial force exerted by the turbine on the flow [19]. Depending on the design of the local turbine controller, one may require a mapping from C_T to the physical turbine settings such as the generator torque and blade pitch angle. This mapping would require the aerofoil tables of the rotor, and possibly higher-fidelity turbine simulations (e.g., using a blade-element-momentum simulation code like FAST [20]) to find the mappings of interest under certain turbine control strategies. Furthermore, the set of (possibly time-varying) model parameters, $\phi_k \in \mathbb{R}^H$, includes the boundary conditions (inflow conditions) and turbulence model properties. The model output is $\mathbf{z}_k \in \mathbb{R}^M$, which typically includes (a subset

of) the states $\mathbf{z}_k \subset \mathbf{x}_k$, and the power production of each turbine inside the farm. Finally, f and g are the nonlinear state forward propagation and output equation, respectively.

WFSim is on the edge of high accuracy and computational tractability for control applications. N typically ranges between $10^3 - 10^4$ for smaller wind farms, resulting in a computational cost of approximately 0.1 s per timestep on a single-core desktop CPU. While this computational load is low compared to LES models, it is very high for controller synthesis. Moreover, the nonlinear nature of WFSim complicates controller synthesis, as many synthesis tools are limited to linear models. On the other hand, this nonlinearity significantly adds to the accuracy of WFSim, and the model attempts to bridge the gap between accuracy and applicability in control.

3. Real-time model calibration

The model calibration solution presented in this work provides estimates of the instantaneous flow field $\hat{\mathbf{x}}_k$ and a subset of the model parameters $\hat{\phi}_k$ using the real-time measurements from the wind turbines. Two steps can be distinguished:

- (i) Estimation of the wind-farm-wide freestream wind speed (U_∞) and direction (WD) is done following the example of [21]. In short, WD is estimated by collecting wind vane measurements of each turbine in the farm, removing outliers, and temporal averaging. For U_∞ , firstly, the non-waked turbines are distinguished from the turbines operating inside a wake using a simplified static wake model [21]. Secondly, the mean power of all upstream turbines is temporally averaged into \bar{P} . This average is used to determine U_∞ using an inversion law derived from actuator disk theory,

$$U_\infty = \sqrt[3]{\frac{2\bar{P}}{C_P A_D \rho}},$$

where C_P is the dimensionless power coefficient of the turbine, A_D is the swept surface area of the rotor, and ρ is the air density.

An important remark is that this methodology for the estimation of U_∞ relies solely on power measurements, and therefore only works for below-rated conditions. For estimation of U_∞ in above-rated conditions, one may, for example, require the implementation of a wind speed estimator on each individual turbine, from which the local wind speed in front of each turbine can be estimated, as demonstrated by [22].

- (ii) The flow field and a subset of model parameters are estimated, extending on previous work [17]. In this work, the extended state vector $\mathbf{s}_k \in \mathbb{R}^{N+1}$ is estimated, where $\mathbf{s}_k^T = [\mathbf{x}_k^T \ \ell_u]$, with $\ell_u \subset \phi_k$ a scalar quantifying the wake recovery in Prandtl's mixing length turbulence model [14]. Specifically, ℓ_u quantifies the slope of the mixing length distance as a function of the downstream distance. The higher ℓ_u , the more wake mixing downstream of each turbine is found in WFSim, and the faster a waked flow recovers to its freestream properties.

Due to nonlinearities in (1), traditional recursive state estimation algorithms such as the linear Kalman filter (KF) cannot be used. Rather, in this work, an Ensemble Kalman filter (EnKF) [23] is opted for, because of its low computational cost and relatively high accuracy for nonlinear models. The EnKF is typically used for large-scale weather forecasting models, which have many similarities with wind farm models. To improve accuracy and cut computational cost, the EnKF has been extended with so-called ‘‘covariance localization’’ and ‘‘covariance inflation’’ in previous work [17].

An important question in the field of state estimation is the system’s observability. Due to the nonlinear nature of WFSim, a formal observability analysis is difficult. Specifically, state observability highly depends on the sensor locations, wind direction, and wind farm layout. However, note that covariance localization is enforced in the EnKF [17], in which the covariance between two spatially distant states is forced to zero. Thus, we intentionally limit the observability by only allowing state updates using spatially nearby sensory information from, e.g., turbine or flow measurements. This not only reduces possible spurious correlations, it also significantly reduces the computational cost. Furthermore, note that not all flow information is equally relevant. In most scenarios, state information in proximity of the turbines is desired, where typically also most sensory information is available. In future work, the usage of more sensory information is envisioned such as the turbine’s structural loads and deformations.

4. A case study

To demonstrate the potential of the calibration algorithm, a case study is performed on a wind farm with two NREL-5MW turbines at 5D spacing, in which the blades are periodically pitched to excite the flow. The blade pitch excitation signal is a pseudorandom binary sequence with values of either 0° or 4° . The turbines are initialized at a 30° yaw misalignment, but are then yawed in alignment with the mean wind direction during the first 20 seconds of the simulation.

The plant in Fig. 1 (“reality”) is modelled by the Simulator fOr Wind Farm Applications (SOWFA), which solves the three-dimensional Navier-Stokes equations accounting for buoyancy and Coriolis effects using a large-eddy simulation [24]. The rotors are represented using the actuator line model. In short, the simulation is of a neutral atmospheric boundary layer with the freestream properties at hub-height being $U_\infty \approx 8$ m/s and $TI_\infty \approx 5\%$. This high-fidelity simulation is described in more detail in [25]. For our purposes, it is assumed that the turbine power signals are the only sensory information available. These measurements are perturbed with artificial Gaussian noise with a standard deviation of $\sigma_P = 2 \cdot 10^4$ W, which is approximately 1.2% and 2.1% of the time-averaged power production for turbine 1 and 2, respectively.

This two-turbine wind farm case is implemented in the WFSim model on a domain of $1.9 \text{ km} \times 0.8 \text{ km}$, spatially discretized at 50×25 cells, and temporally discretized at $\Delta t = 1$ s. The initial extended state vector \hat{s}_0 and freestream wind speed are purposely initialized poorly, to investigate convergence of the estimation algorithm. Specifically, WFSim is initialized with $\ell_{u_0} = 4.0$ and a uniform flow field of 5 m/s. Correspondingly, the freestream wind speed is initialized poorly at $U_{\infty_0} = 5.0$ m/s.

From the turbine power measurements, U_∞ and the extended state vector s_k are to be estimated (WD is ignored for simplicity). The EnKF covariance matrices are largely identical to those in previous work, to simulate the performance for unseen data. Only the measurement covariance noise has been made to match the measurement noise σ_P . For more information on the Kalman filter and its tuning, the reader is referred to [26]. Simulation results are displayed in Figs. 3 and 4.

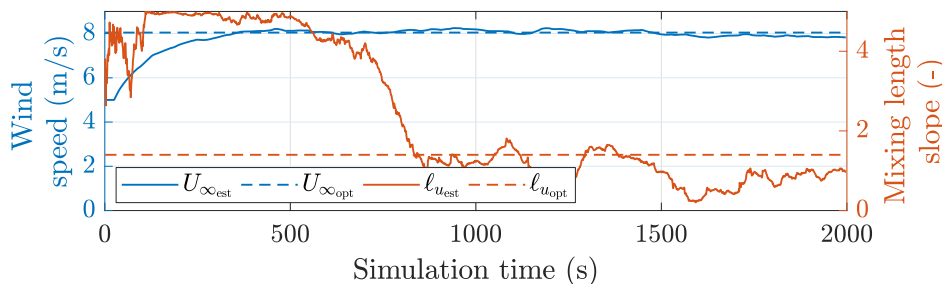


Figure 3: Convergence rates of U_∞ (blue) and ℓ_u (red). In dashed lines are the steady-state values that yield the best fit of WFSim with SOWFA in terms of the flowfields and power signals.

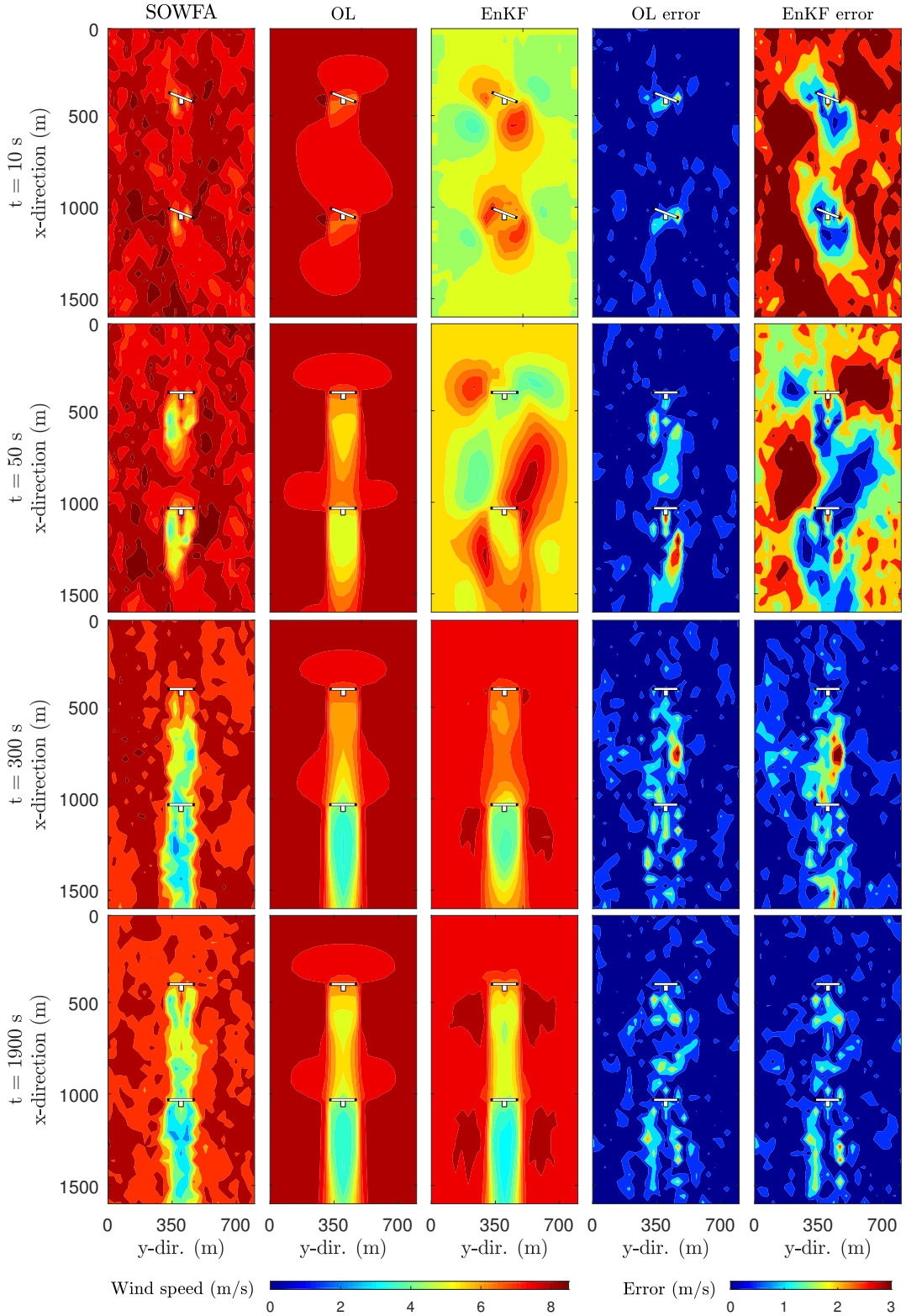


Figure 4: Wind field estimation for $t = 10, 50, 300,$ and 1900 s. In the left column are the large-eddy simulation (SOWFA) results. The second column shows the open-loop (OL) estimation with grid-searched optimal parameters. The third column shows the estimates using power measurements, initialized with poor values for the wind speed and turbulence. The last two columns show the error between the SOWFA and the OL/EnKF simulation, respectively.

Firstly, from Fig. 3, one can see that ℓ_u and U_∞ converge to their steady-state optimal values $\ell_{u_{\text{opt}}}$ and $U_{\infty_{\text{opt}}}$, respectively. These steady-state optimal values have been found through a multi-objective minimization of the error in the flow fields and the error in the turbine power signals of WFSim and SOWFA, thus assuming full state knowledge. Specifically, U_∞ converges to the true wind speed within 400 s, and ℓ_u converges within 850 s. Important to note is that the estimated power production of the downstream turbine can both be influenced by changing the turbulence intensity parameter ℓ_u , or directly by changing the wind speed states in proximity of the turbine. Thus, one may question the observability of the system. However, ℓ_u acts on a much slower timescale than the instantaneous flow field \mathbf{x}_k , and therefore convergence can be achieved.


Secondly, consider Fig. 4. After both parameters have converged ($t = 850$ s) the error between SOWFA and WFSim becomes increasingly smaller. At $t = 1900$ s, the error between SOWFA and the estimate is nearly negligible. Furthermore, as the estimated power capture of each turbine is calculated as a function of the rotor-averaged wind speed at the rotor plane, there is a direct relationship (correlation) between these flow states and the power capture. Thus, using power measurements, these flow states on the rotor plane undergo the most dominant corrections, and it can be seen that the turbine power measurements most immediately affect the wind speed estimates in proximity of the turbines.

In terms of computational cost, each state estimate takes approximately 1.0 s on an Intel i7-6600U dual-core CPU for one single forward timestep, up to two orders of magnitude faster than common KF algorithms [16]. In comparison, the open-loop simulations with WFSim take approximately 0.03 s per timestep on a single core.

5. Conclusion

In this work, we presented an algorithm for real-time joint state-parameter estimation in low- and medium-fidelity dynamical wind farm models. In a high-fidelity simulation, we demonstrated that the local flow field, local turbulence, and freestream wind speed can jointly be estimated for a two-turbine wind farm using exclusively SCADA data, at a low computational cost of 1.0 s per timestep on an Intel i7-6600U dual-core CPU. We used an Ensemble Kalman filter for its computational efficiency and its ability to deal with nonlinearities. This state and model parameter information can now be leveraged in algorithms relying on the WFSim model for robust and accurate wind farm optimization. A future publication will include a comparison of the EnKF with other nonlinear KF variants, an investigation of the effect of information source on the estimation quality, and simulations on a nine-turbine wind farm [26]. Furthermore, future work may include an analysis of the estimation performance under a changing wind direction, and possibly the incorporation of additional sensory information.

Acknowledgements

We thank Matti Morzfeld, Torben Knudsen, and Paul Fleming for their contributions in this work. However, any errors in this work remain our own. The authors would like to acknowledge the CL-Windcon project. This project has received funding from the European Union’s Horizon 2020 research and innovation programme under grant agreement No 727477.  Support from the Hanse-Wissenschaftskolleg, Delmenhorst, Germany is also gratefully acknowledged.

Code availability

All models and algorithms presented in this article are open-source. The surrogate wind farm model (WFSim) and the calibration solution are available in the public domain at <https://github.com/TUdelft-DataDrivenControl/>. SOWFA is available at <https://github.com/NREL/SOWFA>. All rights for SOWFA go to the National Renewable Energy Laboratory (NREL) for performing the simulation and providing the data.

References

- [1] International Energy Agency (IEA) 2017 World energy outlook Tech. rep. International Energy Agency (IEA)
- [2] International Monetary Fund (IMF) 2017 World economic outlook Tech. rep. International Monetary Fund (IMF) Washington D.C., USA
- [3] Boersma S, Doekemeijer B, Gebraad P, Fleming P, Annoni J, Scholbrock A, Frederik J and van Wingerden J W 2017 A tutorial on control-oriented modeling and control of wind farms *American Control Conference* (Seattle, USA) pp 1–18
- [4] Barthelmie R J, Pryor S C, Frandsen S T, Hansen K S, Schepers J G, Rados K, Schlez W, Neubert A, Jensen L E and Neckelmann S 2010 Quantifying the impact of wind turbine wakes on power output at offshore wind farms *Journal of Atmospheric and Oceanic Technology* **27** 1302–1317
- [5] Gebraad P M O, Teeuwisse F W, van Wingerden J W, Fleming P A, Ruben S D, Marden J R and Pao L Y 2016 Wind plant power optimization through yaw control using a parametric model for wake effects—a CFD simulation study *Wind Energy* **19** 95–114
- [6] Goit J P, Munters W and Meyers J 2016 Optimal coordinated control of power extraction in LES of a wind farm with entrance effects *Energies* **9**
- [7] Bastankhah M and Porté-Agel F 2016 Experimental and theoretical study of wind turbine wakes in yawed conditions *Journal of Fluid Mechanics* **806** 506–541
- [8] Campagnolo F, Petrović V, Bottasso C L and Croce A 2016 Wind tunnel testing of wake control strategies *American Control Conference* (Boston, USA) pp 513–518
- [9] Campagnolo F, Petrović V, Schreiber J, Nanos E M, Croce A and Bottasso C L 2016 Wind tunnel testing of a closed-loop wake deflection controller for wind farm power maximization *Journal of Physics: Conference Series* **753**
- [10] Fleming P, Annoni J, Shah J J, Wang L, Ananthan S, Zhang Z, Hutchings K, Wang P, Chen W and Chen L 2017 Field test of wake steering at an offshore wind farm *Wind Energy Science* **2** 229–239
- [11] van Wingerden J W, Pao L Y, Aho J and Fleming P A 2017 Active power control of waked wind farms *IFAC World Congress* vol 50 (Toulouse, France) pp 4484–4491
- [12] Shapiro C, Meyers J, Meneveau C and Gayme D F 2018 Coordinated pitch and torque control of wind farms for power tracking *American Control Conference* (Milwaukee, USA)
- [13] Siniscalchi-Minna S, Bianchi F D and Ocampo-Martinez C 2018 Predictive control of wind farms based on lexicographic minimizers for power reserve maximization *American Control Conference* (Milwaukee, USA)
- [14] Boersma S, Doekemeijer B, Vali M, Meyers J and van Wingerden J W 2018 A control-oriented dynamic wind farm model: WFSim *Wind Energy Science* **3** 75–95
- [15] Vali M, van Wingerden J W, Boersma S, Petrović V and Kühn M 2016 A predictive control framework for optimal energy extraction of wind farms *Journal of Physics: Conference Series* **753**
- [16] Doekemeijer B M, van Wingerden J W, Boersma S and Pao L Y 2016 Enhanced Kalman filtering for a 2D CFD NS wind farm flow model *Journal of Physics: Conference Series* **753**
- [17] Doekemeijer B M, Boersma S, Pao L Y and van Wingerden J W 2017 Ensemble Kalman filtering for wind field estimation in wind farms *American Control Conference* (Seattle, USA) pp 19–24
- [18] Iungo G V, Santhanagopalan V, Ciri U, Viola F, Zhan L, Rotea M A and Leonardi S 2018 Parabolic RANS solver for low-computational-cost simulations of wind turbine wakes *Wind Energy* **21** 184–197
- [19] Munters W and Meyers J 2017 An optimal control framework for dynamic induction control of wind farms and their interaction with the atmospheric boundary layer *Philosophical Transactions of the Royal Society of London A: Mathematical, Physical and Engineering Sciences* **375**
- [20] Jonkman J M and Jonkman B J 2016 FAST modularization framework for wind turbine simulation: full-system linearization *Journal of Physics: Conference Series* **753**
- [21] Mittelmeier N, Blodau T and Kühn M 2017 Monitoring offshore wind farm power performance with SCADA data and an advanced wake model *Wind Energy Science* **2** 175–187
- [22] Simley E and Pao L Y 2016 Evaluation of a wind speed estimator for effective hub-height and shear components *Wind Energy* **19** 167–184
- [23] Evensen G 2003 The ensemble Kalman filter: theoretical formulation and practical implementation *Ocean Dynamics* **53** 343–367
- [24] Fleming P, Gebraad P, Lee S, van Wingerden J W, Johnson K, Churchfield M, Michalakes J, Spalart P and Moriarty P 2014 Evaluating techniques for redirecting turbine wakes using SOWFA *Renewable Energy* **70** 211 – 218
- [25] Annoni J, Gebraad P and Seiler P 2016 Wind farm flow modeling using an input-output reduced-order model *American Control Conference* (Boston, USA) pp 506–512
- [26] Doekemeijer B M, Boersma S, Pao L Y, Knudsen T and van Wingerden J W 2018 Online model calibration for a simplified LES model in pursuit of real-time closed-loop wind farm control *Wind Energ. Sci. Discuss.* **2018** in preparation